Enigmatic textures developed along plagioclase-augite grain boundaries at the base of the Main Zone, Northern Limb, Bushveld Complex - Evidence for late stage melt infiltration int...

Article *in* South African Journal of Geology · July 2009

DOI: 10.2113/gssajg.112.1.39

4 authors:

Freddie Roelofse
University of the Free State

L.D. Ashwal
University of the Witwatersrand

Carlos Pineda-Vargas
iThemba Labs - Laboratory for Accelerator Based Science

Wojciech J Przybyłowicz
AGH University of Science and Technology in Kraków

Enigmatic textures developed along plagioclase-augite grain boundaries at the base of the Main Zone, Northern Limb, Bushveld Complex – evidence for late stage melt infiltration into a nearly solidified crystal mush

F. Roelofse
Council for Geoscience, Private Bag X112, Pretoria, 0001
e-mail: froelofse@geoscience.org.za

L.D. Ashwal
School of Geosciences, University of the Witwatersrand, Private Bag 3, WITS, 2050
e-mail: ashwall@geosciences.wits.ac.za

C.A. Pineda-Vargas
Materials Research Group, iThemba LABS, PO Box 722, Somerset West, 7129
Faculty of Health and Wellness Sciences, Cape Peninsula University of Technology, Bellville, South Africa
e-mail: pineda@tlabs.ac.za

W.J. Przybylowicz
Materials Research Group, iThemba LABS, PO Box 722, Somerset West, 7129
On leave from: Faculty of Physics and Applied Computer Science,
AGH University of Science and Technology, Kraków, Poland
e-mail: przybylowicz@tlabs.ac.za

ABSTRACT

An enigmatic texture in which orthopyroxene exsolution lamellae within clinopyroxene protrude into adjacent plagioclase crystals occurs in a gabbronorite occurring at the base of the Main Zone in the Northern Sector of the Northern Limb of the Bushveld Complex. Grain boundaries exhibiting this texture are characterised by plagioclase richer in An component and clinopyroxene with higher Mg# in comparison to the bulk of the plagioclase and clinopyroxene, respectively. The texture is interpreted as representing the products formed during late-stage infiltration of a more primitive magma into a nearly solidified crystal mush, with concomitant displacement of the last dregs of intercumulus melt. A solid-state origin for the texture appears untenable, as does derivation of the infiltrating melt from the underlying Platreef.

Introduction

In this contribution we describe some enigmatic textures developed along plagioclase-augite grain boundaries present in gabbronorite at the base of the Main Zone in the Northern Sector of the Northern Limb of the Bushveld Complex, as exposed by the 1563.02 m deep MO-1 drill hole drilled on the farm Moordkopje 813LR. The hole is collared in Main Zone rocks and intersects ~1350 m of Main Zone gabbros, norites, gabbronorites and anorthosites. The Main Zone in the core is underlain by ~150 m of orthopyroxene-rich cumulates of the Platreef, which is in turn underlain by a package of hybridised rocks thought to have formed as a result of contamination with the underlying granite footwall (Roelofse and Ashwal, 2008). The textures forming the focus of this paper occur in a narrow zone of gabbronorite perhaps as much as 15 m thick, from a depth of 1346 m.

Petrography

The rock in which the texture is preserved is a medium- to coarse grained gabbronorite consisting of approximately 60% plagioclase, much of which has been altered to a mixture of fine-grained, brownish minerals (probably epidote, chlorite, smectite and amphibole (Roelofse and Ashwal, 2008)). Clinopyroxene dominates over orthopyroxene, and quartz, amphibole, biotite, talc and opaques occur as accessory phases. The texture of the rock can best be described as ophitic to poikilophitic in that locally, laths of plagioclase occur enclosed or partially enclosed within 'large', optically continuous oikocrysts of clinopyroxene (Figure 1). Elsewhere however, both plagioclase and orthopyroxene occur enclosed or partially enclosed within clinopyroxene oikocrysts. Orthopyroxene typically contains an abundance of thin, closely spaced clinopyroxene exsolution lamellae, whereas clinopyroxene typically contains thicker, more widely spaced orthopyroxene exsolution lamellae. The enigmatic texture forming the focus of this paper is developed along plagioclase clinopyroxene grain boundaries and consists of orthopyroxene exsolution lamellae within clinopyroxene oikocrysts protruding up to ~10 micron into adjacent plagioclase laths (Figure 2). A fairly

doi:10.2113/gssajg.112.1.39

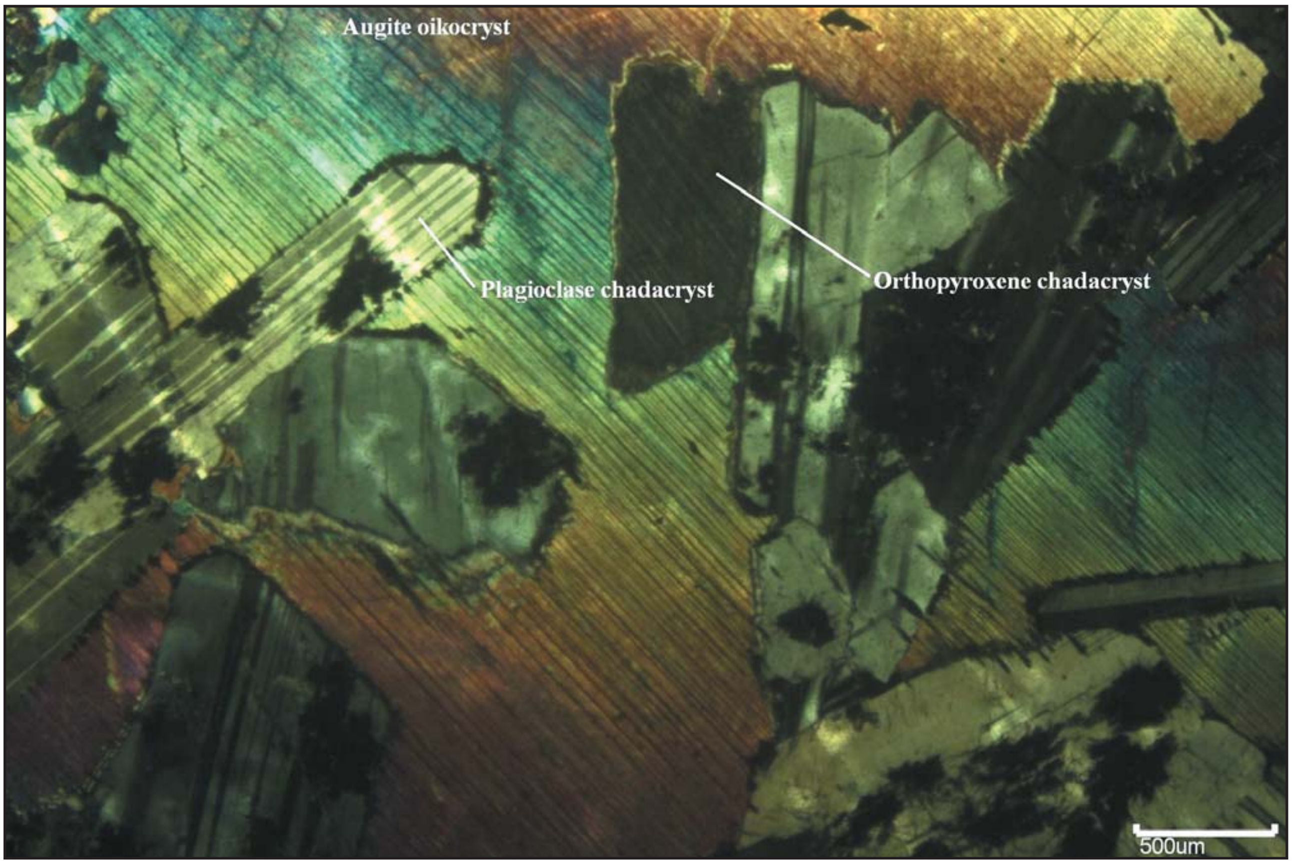

Figure 1. Photomicrograph showing poikilophitic texture as developed in the gabbronorite in which the texture forming the focus of this paper occurs. Cross polarised light.

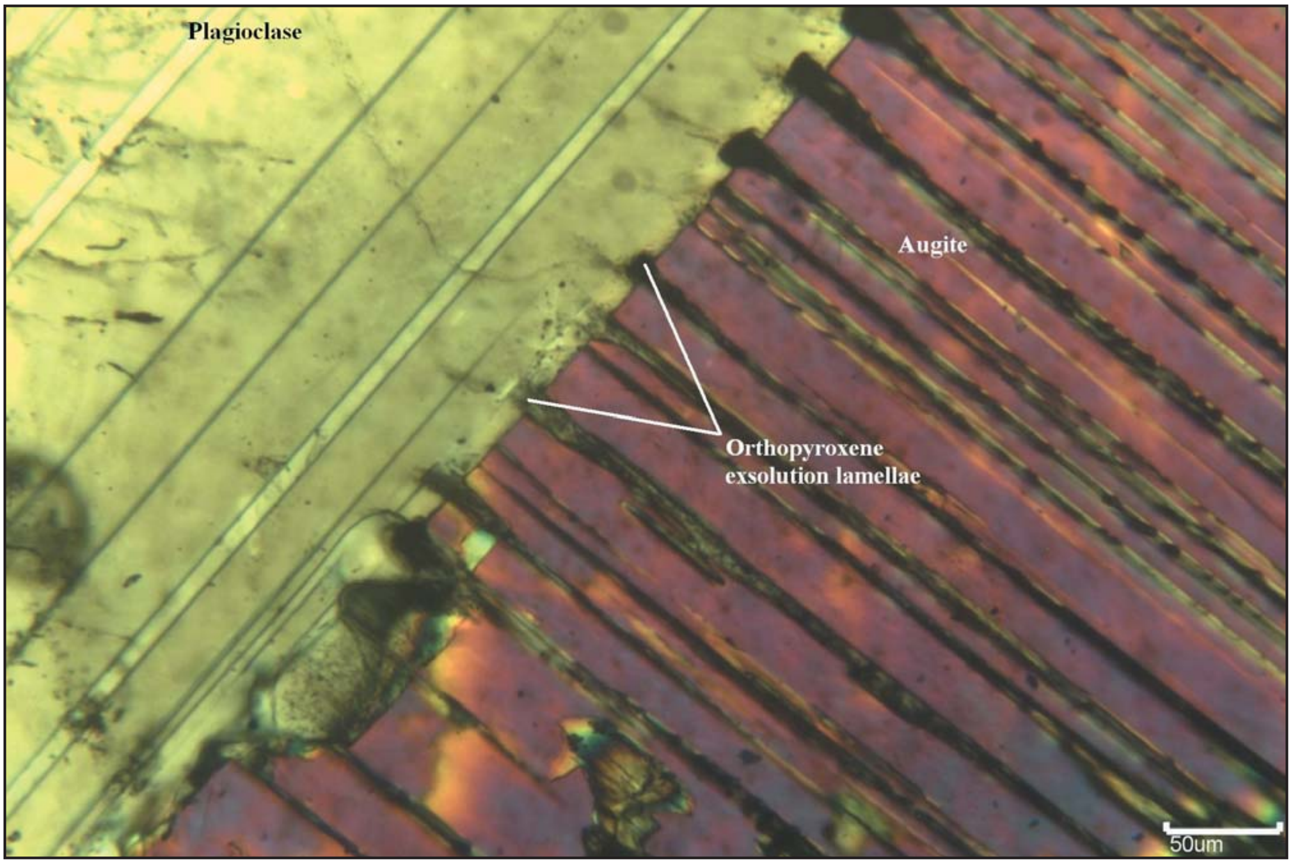

Figure 2. Photomicrograph showing orthopyroxene exsolution lamellae in augite protruding into adjacent plagioclase grain. Note the widening of the exsolution lamellae as the grain boundary is approached from the augite side. Cross polarised light.

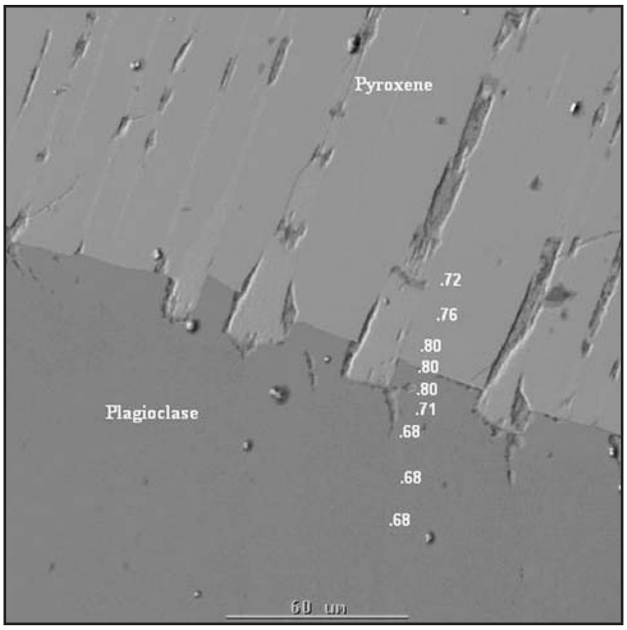

Figure 3. Back-scattered electron image showing orthopyroxene exsolution lamellae within clinopyroxene protruding into adjacent plagioclase grain. Note the gradual widening of exsolution lamellae towards the grain boundary and the stepped nature of the grain boundary itself. Numbers represent the An content of plagioclase and Mg# of clinopyroxene as determined by electron microprobe.

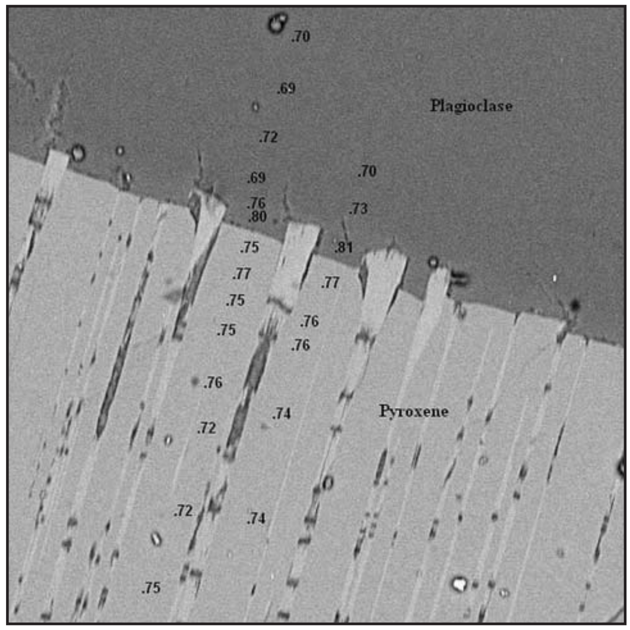

Figure 4. Back-scattered electron image showing the variation in An content of plagioclase and Mg# of clinopyroxene in two line profiles conducted across grain boundaries exhibiting the texture forming the focus of this paper. Width of field of view ~250 micron.

common feature of the orthopyroxene exsolution lamellae at these grain boundaries is a gradual widening by as much as 100% as the grain boundary is approached from the clinopyroxene side. Another common feature of the grain boundaries showing this texture is that the interfaces between plagioclase and clinopyroxene occurring between adjacent orthopyroxene exsolution lamellae are stepped, convex or concave rather than straight (Figure 3).

Methodology

Mineral compositions of plagioclase, clinopyroxene and orthopyroxene exsolution lamellae in the vicinity of grain boundaries exhibiting the texture described above were determined using energy dispersive X-ray spectrometry using the Jeol 733 Superprobe of the University of Johannesburg, calibrated with relevant oxide standards. An accelerating voltage of 15 kV, a beam current of 6.4 nA and a focused beam was used for the analyses, which included a number of line profiles across grain boundaries exhibiting this texture. The texture was also studied using the Council for Geoscience's Leica 440 Stereoscan scanning electron microscope equipped with an Inca (Oxford) energy dispersive spectrometer. Analyses were performed at counting times of 50 seconds, a beam current of 5nA and an accelerating voltage of 20kV.

Elemental mapping and point analyses along selected line profiles were performed using the nuclear microprobe at the Materials Research Group, iThemba LABS (Prozesky *et al.* 1995). PIXE (Particle Induced X-ray Emission) spectra were registered using a Si(Li) energy dispersive detector manufactured by PGT (30 mm^2 active area, energy resolution ca. 160 eV at 5.9 keV). A proton beam of 1.6 MeV energy, current ~50 pA and focused to a spot size of 5 x 3 μm^2 was used. The selection of the proton beam energy was dictated by

Table 1. Compositions of individual spots analysed by electron microprobe for the line profile shown in Figure 3.

Al_2O_3	CaO	FeO	K_2O	MgO	MnO	Na_2O	SiO_2	TiO_2	Total	An%/ Mg#
30.18	13.86	–	0.31	–	–	3.58	51.12	–	99.05	**68**
30.67	13.87	–	0.48	–	–	3.61	51.47	–	100.10	**68**
30.63	13.67	0.49	–	–	–	3.51	51.14	–	99.44	**68**
30.99	14.42	0.44	–	–	–	3.25	50.24	–	99.34	**71**
32.85	16.25	0.43	–	–	–	2.22	48.33	–	100.08	**80**
32.30	15.79	0.57	–	–	–	2.19	47.78	–	98.63	**80**
0.99	23.49	6.72	–	14.83	0.43	0.34	52.46	0.33	99.59	80
1.33	22.51	8.08	–	14.62	–	–	52.20	0.36	99.10	76
1.22	19.79	10.9	–	15.51	–	–	52.33	–	99.75	72

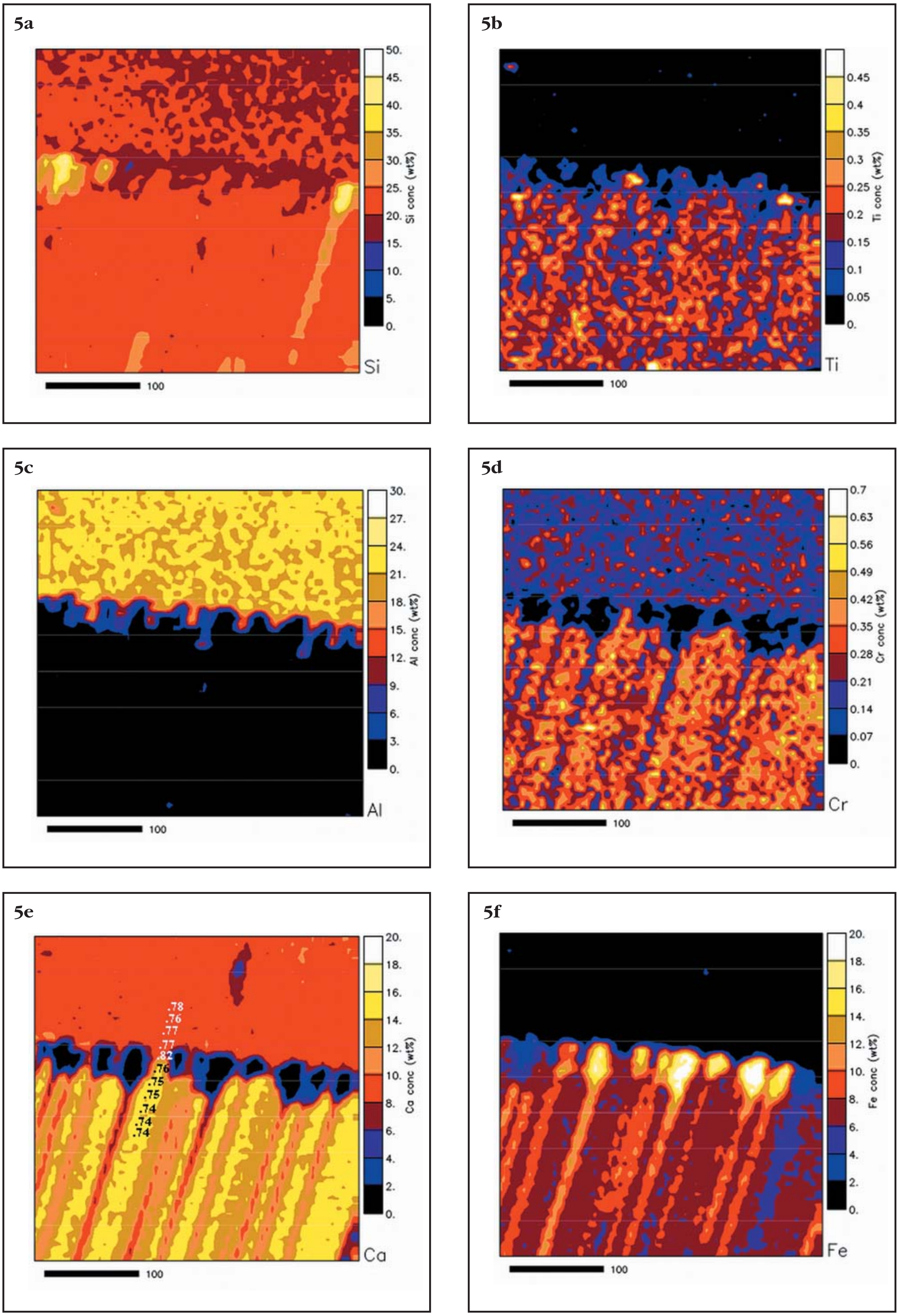
5a
50.
45.
40.
35.
30.
25.
20.
15.
10.
5.
0.
Si conc (wt%)
Si
100
5b
0.45
0.4
0.35
0.3
0.25
0.2
0.15
0.1
0.05
0.
Ti conc (wt%)
Ti
100
5c
30.
27.
24.
21.
18.
15.
12.
9.
6.
3.
0.
Al conc (wt%)
Al
100
5d
0.7
0.63
0.56
0.49
0.42
0.35
0.28
0.21
0.14
0.07
0.
Cr conc (wt%)
Cr
100
5e
.78
.76
.77
.77
.82
.76
.75
.75
.74
.74
.74
20.
18.
16.
14.
12.
10.
8.
6.
4.
2.
0.
Ca conc (wt%)
Ca
100
5f
20.
18.
16.
14.
12.
10.
8.
6.
4.
2.
0.
Fe conc (wt%)
Fe
100

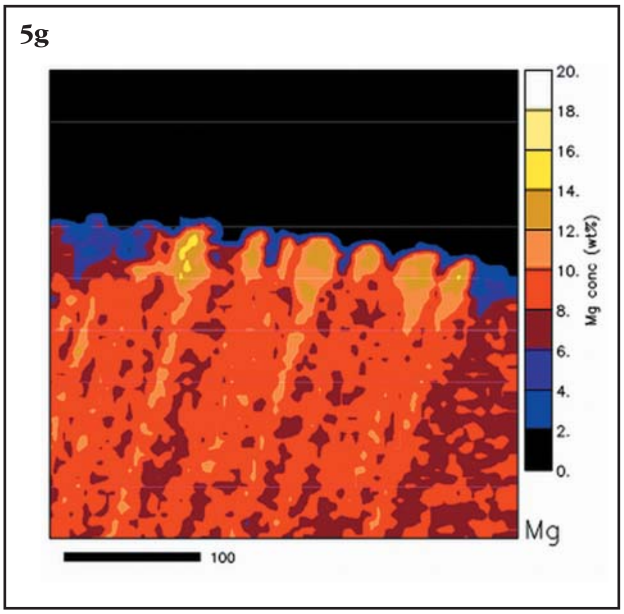

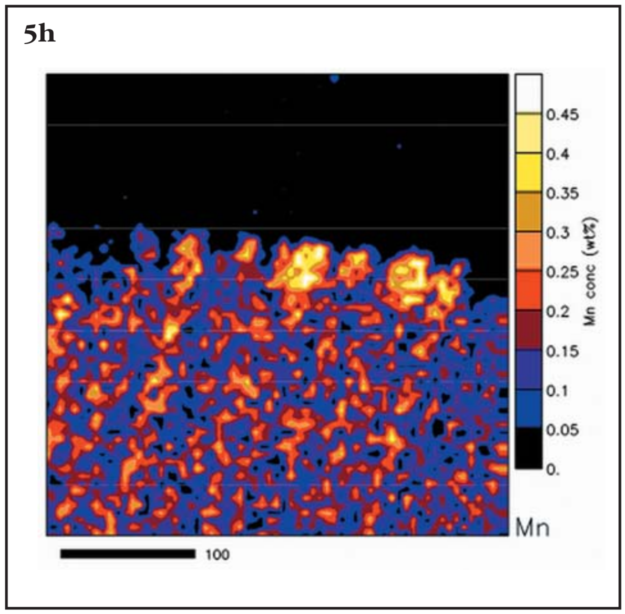

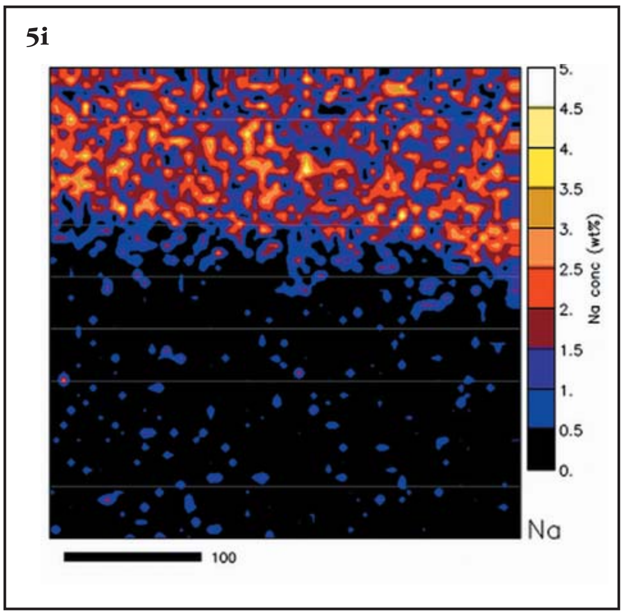

Figure 5. PIXE elemental maps showing the spatial variation in concentration for a number of elements in the vicinity of a grain boundary exhibiting the texture discussed in this paper. Numbers on the map for Ca represent the An content of plagioclase (shown in white) and the Mg# of clinopyroxene (shown in black) as determined in a line profile conducted using the nuclear microprobe. Note the decrease and increase in the concentrations of silicon and calcium in plagioclase, respectively, as the grain boundary is approached.

the thickness of specimens; as the maximum energy at which protons would be stopped completely within the specimen, without hitting the glass substrate. A beryllium absorber (thickness 25 μm) was used to prevent backscattered protons from hitting the detector crystal. Quantitative elemental maps were obtained by scanning the proton beam across the selected areas, storing data in list mode, and next processing them off-line using the dynamic analysis method, which forms an integral part of the GeoPIXE II software (Ryan, 2000). PIXE data from point analyses were processed using a full nonlinear deconvolution procedure, and complemented the information obtained from the maps.

Results

Electron microprobe analyses (Table 1) indicate an increase in the anorthite content of the plagioclase situated along clinopyroxene grain boundaries and between orthopyroxene lamellae from background values of around 65% An away from the grain boundary to around 80% An at the grain boundary (Figure 4). Clinopyroxene shows an analogous increase in its Mg# (molar 100Mg/(Mg+Fe)) from background values on the order of 72 up to a maximum of 80 at its grain boundaries with plagioclase. The increase in the Mg# of clinopyroxene as the grain boundary with plagioclase is approached is considerably more gradual than the corresponding increase in the anorthite content of plagioclase, with a consistent increase in the Mg# typically coinciding with the gradual widening of orthopyroxene exsolution lamellae towards the grain boundary. Clinopyroxene compositions as determined by energy dispersive X-ray spectrometry using the SEM as described above similarly showed a higher Mg# for rim material (76.2 ± 0.7; n = 8) in comparison to non-rim material (74.4 ± 1.1; n = 19), with the difference between the two sample sets being statistically significant (t-statistic = 4.49; degrees of freedom = 25; p-value = 0.05).

PIXE maps for most elements did not succeed in visually resolving the zonation in An% of plagioclase and Mg# of clinopyroxene at the grain boundaries showing this texture. Elemental maps for Ca and Si, however, show a slight increase and decrease in concentration in plagioclase along affected grain boundaries, respectively, as also seen in the line profiles conducted using the EMP and NMP (Figure 5). Although the elemental maps for Al and Na did not visually

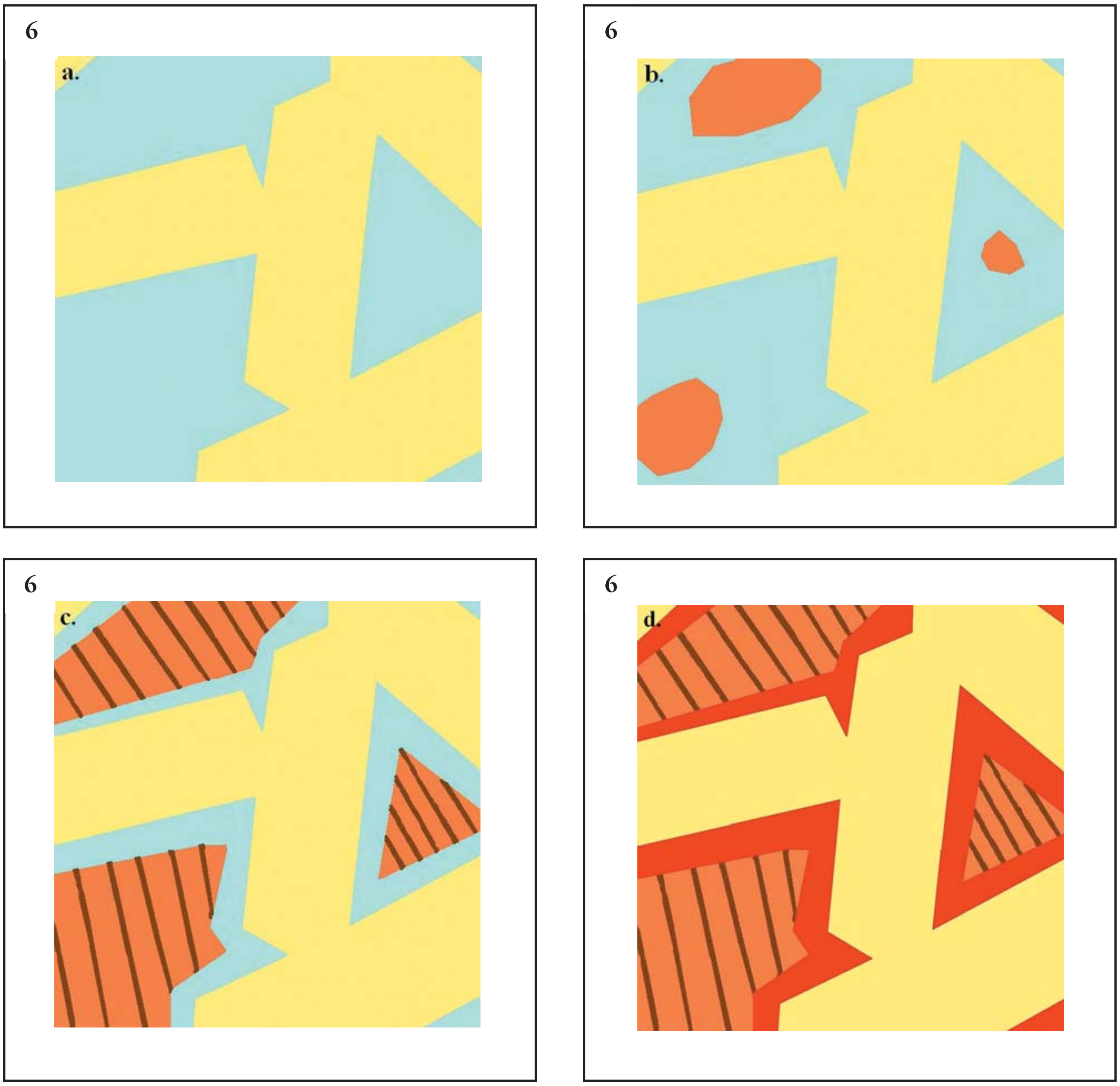

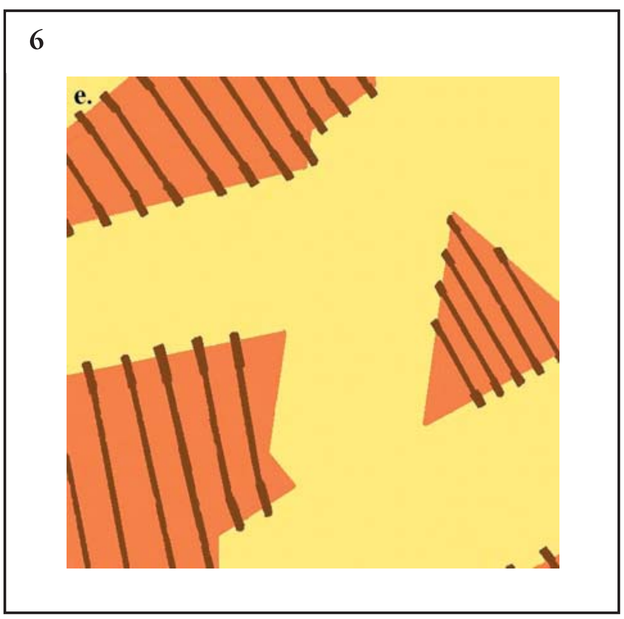

Figure 6. Schematic representation of the sequence of events thought to have occurred in the development of the texture. See text for details. (Yellow = plagioclase, cyan =original interstitial melt, orange = clinopyroxene, brown = orthopyroxene, red = newly infiltrated more primitive melt).

resolve any zonation at the grain boundaries, both the EMP and NMP showed an increase and decrease, respectively, in their concentrations as the grain boundary is approached from the plagioclase side, which is in agreement with the well known plagioclase substitution reaction CaAl ↔ NaSi (Morse and Nolan, 1984).

Discussion

Plagioclase exhibiting reversed rims is a fairly common feature of cumulate rocks, having been described from a number of intrusions, *e.g.* the Kiglapait intrusion (Morse and Nolan, 1984), the Bushveld Complex (Harney *et al.*,

1990) and the St. Urbain massif (Dymek, 1981). A number of mechanisms have been proposed to account for plagioclase exhibiting reversed rims, including the crystallization of intercumulus liquid (Morse and Nolan, 1984), an increase in the P_{H2O} of interstitial melt as a result of the early crystallisation of anhydrous phases (Von Gruenewaldt, 1971), hydrothermal infiltration metasomatism (Schiffries, 1982) and retrograde pyroxene-plagioclase equilibration upon cooling (Dymek, 1981). However, none of these mechanisms can adequately explain the concomitant increase in the Mg# of clinopyroxenes where they are in contact with plagioclase exhibiting reversed rims and the protrusion of orthopyroxene exsolution lamellae within clinopyroxene into adjacent plagioclase.

Textures reminiscent of the features described here occur within the Skaergaard intrusion, in which augite 'hooks' protrude into adjacent An-rich plagioclase. Such textures have been attributed to the preferential growth of augites containing orthopyroxene exsolution lamellae at the expense of the exsolution lamellae themselves (Holness *et al.*, 2007) and if developed fully, the plagioclase-augite grain boundaries are transformed into a symplectite consisting of vermicular augite within An-rich plagioclase. Similar symplectites have been described from gabbros from the Mathematician Ridge in the Eastern Pacific, with infiltration of primitive magma through a crystal mush being cited as a possible explanation for the genesis of this texture (Batiza and Vanko, 1985). We propose that the texture described in this paper formed in an analogous manner, as will be discussed below.

Other textures reminiscent of that described in this paper were reported upon by Zingg (1996), working on norites of the Western Limb of the Bushveld Complex in the interval between the UG-2 chromitite and the Merensky Reef, where parallel biotite plates tracing the (100) direction of adjacent orthopyroxene occur within plagioclase. The anhedral nature of orthopyroxene in these rocks was interpreted as the corrosion of orthopyroxene with concomitant overgrowth by plagioclase, with the parallel biotite plates reflecting the original position of exsolution lamellae within the host orthopyroxene and with the reaction being driven by transfer of matter as a result of a fluid gradient. A similar origin for the texture described in this paper is unlikely, due to the absence of hydrous phases such as biotite and amphibole within the grain boundary areas between plagioclase and clinopyroxene.

We propose that the texture under consideration here formed by the infiltration of a more primitive melt into the nearly solidified cumulate pile, which in the process displaced the intercumulus liquid still present within the crystal mush. The following sequence of events is proposed to account for the observations:

- The ophitic texture of parts of the rock in which apparently cumulus plagioclase laths occur partially enclosed by supposedly intercumulus clinopyroxene suggests that plagioclase predates clinopyroxene and that originally, plagioclase would have formed a cumulus network within surrounding interstitial melt (Figure 6a).
- Additional cooling would have resulted in the crystallisation of clinopyroxene within pools of interstitial melt (Figure 6b).
- The intercumulus clinopyroxene will grow in size as cooling proceeds and orthopyroxene exsolution lamellae form within the clinopyroxene (Figure 6c) before the rock has undergone complete solidification.
- A more primitive melt capable of crystallising orthopyroxene, An-rich plagioclase and clinopyroxene with a higher Mg# infiltrates the partially solidified crystal mush, displacing the last dregs of intercumulus melt (Figure 6d).
- The newly infiltrated melt is initially saturated with respect to orthopyroxene, which nucleates onto the pre-existing orthopyroxene exsolution lamellae within clinopyroxene, resulting in the broadening and lengthening of the lamellae. Subsequent cooling results in the crystallisation of plagioclase enriched in An component and clinopyroxene with an elevated Mg# adjacent to the broadened orthopyroxene lamellae (Figure 6e).

A solid-state process for the formation of the textures was also considered, but rejected based on the available evidence. Plagioclase is known to dissolve in high Ca-pyroxene at elevated pressures according to the reactions:

$$CaMgSi_2O_6 + xNaAlSi_3O_8 \rightarrow CaMgSi_2O_6.xNaAlSi_2O_6 + xSiO_2$$
$$CaMgSi_2O_6 + xCaAl_2Si_2O_8 \rightarrow CaMgSi_2O_6.xCaAl_2SiO_6 + xSiO_2$$

Kushiro (1969) has shown that at constant temperature, the ability of pyroxene to dissolve plagioclase according to the above reactions increases with increasing pressure, whereas, at constant pressure, the ability of pyroxene to dissolve plagioclase increases with decreasing temperature. The absence of an identifiable source of silica, which would be required for the reverse reaction as shown above, argues against an 'exsolution'

Table 2. Comparison between the chemical composition of the Platreef in contact with the Main Zone as determined by x-Ray fluorescence analysis and the estimated composition of the grain boundary area exhibiting this texture.

	Uppermost Platreef	Grain boundary area
SiO_2	49.86	50.2
Al_2O_3	8.34	16.8
Cr_2O_3	0.37	–
CaO	6.31	19.5
MgO	20.28	7.4
FeO	9.90	4.0
Na_2O	0.50	1.2
TiO_2	0.12	0.2
MnO	0.19	0.1

origin for the plagioclase occurring at the grain boundaries exhibiting this texture. Furthermore, the pressures required to dissolve appreciable amounts of plagioclase in pyroxene at magmatic temperatures are considerably higher than the pressure (~4 kb) at which these rocks are thought to have formed (Nell, 1985). A solid-state origin for these textures therefore appears untenable.

A problem that cannot be satisfactorily addressed at this stage is why the texture as described above is not more common within the Bushveld Complex but instead seemingly confined to the immediate hangingwall to the Platreef. A possibility considered but rejected based on firm evidence to the contrary (Holwell *et al.*, 2005; Holwell and Jordaan, 2006) is that the Platreef may have postdated the Main Zone and that the Platreef magma may have been the source of the melt that infiltrated the overlying Main Zone crystal mush. A further possibility would be that the intruding Main Zone magma may have partially molten the underlying Platreef footwall, with the infiltrating melt perhaps representing a portion of molten Platreef percolating upwards through the crystallizing crystal mush.

The composition of the uppermost Platreef as preserved in the Moordkopje drill core is presented in Table 2, along with the estimated composition of the grain boundary area as estimated from back-scattered electron images and electron microprobe analyses. The differences between the compositions of the uppermost Platreef melagabbronorite and the inferred grain boundary composition suggest that melt derived from the melting of Platreef must have mixed with melt already interstitially present within the crystal mush in order to account for the observed composition of the grain boundary area. However, if a melt generated by melting of the underlying Platreef is cited as a source for the melt thought to have infiltrated the crystal mush in which the texture occurs, one might expect that such a melt would have interacted with the crystallising Main Zone magma early during its crystallisation history and not during the very latest stages as is suggested by the textural evidence presented here.

Nevertheless, there exists ample evidence for late-stage melt migration within the Bushveld Complex and specifically within the basal parts of the Main Zone (Mitchell *et al.*, 1998 and references therein), although textural evidence thereof as presented here, may not necessarily be everywhere preserved due to subsolidus processes. In-situ isotopic studies may be useful in testing our present hypothesis for the genesis of this texture, on the assumption that the isotopic composition of the proposed infiltrating magma was different from that of the original magma from which the bulk of the rock crystallised.

Acknowledgements

FR would like to thank the CEO of the Council for Geoscience, for allowing the results to be published and for financially supporting the project, whilst Anglo Platinum is thanked for allowing access to the drill core. The constructive criticism by Paul Buchanan and an anonymous reviewer is also greatly acknowledged.

References

Batiza, R. and Vanko, D.A. (1985). Petrologic evolution of large failed rifts in the Eastern Pacific: Petrology of volcanic and plutonic rocks from the Mathematician Ridge area and the Guadalupe Trough. *Journal of Petrology,* **26**, 564-602.

Dymek, R.F. (1981). Reverse zoning in plagioclase from labradorite anorthosite, St. Urbain massif, Quebec: retrograde plag-pyx reaction? *Geological Society of America Abstracts With Programme,* **13**, 444.

Harney, D.M.W., Merkle, R.K.W., Von Gruenewaldt, G. (1990). Plagioclase composition in the Upper Zone, Eastern Bushveld Complex – support for magma mixing at the Main Magnetite Layer. *Institute for Geological Research on the Bushveld Complex Research Report*, **87**, 19pp.

Holness, M.B., Tegner, C., Nielsen, T.F.D., Stripp, G., Morse, S.A. (2007). A textural record of solidification and cooling in the Skaergaard Intrusion, East Greenland. *Journal of Petrology,* **48**, 2359-2377.

Holwell, D.A., Armitage, P.E.B., McDonald, I. (2005). Observations on the relationship between the Platreef and its hangingwall. *Transactions of the Institute of Mining and Metallurgy B,* **114**, 199-207.

Holwell, D.A., Jordaan, A. (2006). Three-dimensional mapping of the Platreef at the Zwartfontein South Mine: implications for the timing of magmatic events in the northern limb of the Bushveld Complex, South Africa. *Transactions of the Institute of Mining and Metallurgy B,* **115**, 41-48.

Kushiro, L. (1969). Clinopyroxene solid solutions formed by reactions between diopside and plagioclase at high pressures. *Mineralogical Society of America Special Paper*, **2**, 179-191.

Mitchell, A.A., Eales, H.V., Kruger, F.J. (1998). Magma replenishment and the significance of poikilitic textures in the Lower Main Zone of the western Bushveld Complex, South Africa. *Mineralogical Magazine,* **62**, 435-450.

Morse, S.A. and Nolan, K.M. (1984). Origin of strongly reversed rims on plagioclase in cumulates. *Earth and Planetary Science Letters,* **68**, 485-498.

Nell, J. (1985). The Bushveld metamorphic aureole in the Potgietersrus area: evidence for a two-stage metamorphic event. *Economic Geology,* **80**, 1129-1152.

Prozesky VM, Przybylowicz WJ, Van Achterbergh E, Churms CL, Pineda CA, Springhorn KA, Pilcher JV, Ryan CG, Kritzinger J, Schmitt H, T. Swart (1995). The NAC nuclear microprobe facility. *Nuclear Instruments and Methods in Physics Research B* 104: 36-42.

Roelofse, F. and Ashwal, L.D. (2008). Symplectitic augite from the Platreef – textural evidence for fluid/rock interaction in the Northern Sector of the Northern Limb of the Bushveld Complex? *South African Journal of Geology,* **111,** 21-26.

Ryan CG (2000). Quantitative trace element imaging using PIXE and the nuclear microprobe. *International Journal of Imaging Systems and Technology,* **11**, 219-230.

Schiffries, C.M. (1982). The petrogenesis of a platiniferous dunite pipe in the Bushveld Complex: infiltration metasomatism by a chloride solution. *Economic Geology,* **77**, 1439-1453.

Von Gruenewaldt, G. (1971). A petrological and mineralogical investigation of the rocks of the Bushveld Igneous Complex in the Tauteshoogte-Roossenekal area of the eastern Transvaal. PhD thesis, University of Pretoria (unpublished).

Zingg, A.J. (1996). Recrystallization and the origin of layering in the Bushveld Complex. *Lithos,* **37**, 15-37.

Editorial handling: J. M. Barton